PHYSICAL REVIEW B **83**, 134506 (2011)

Mixed-state Hall effect and flux pinning in $Ba(Fe_{1-x}Co_x)_2As_2$ single crystals ($x = 0.08$ and 0.10)

L. M. Wang,[1,*] Un-Cheong Sou,[1] H. C. Yang,[1,†] L. J. Chang,[2,3] Cheng-Maw Cheng,[4] Ku-Ding Tsuei,[4] Y. Su,[5] Th. Wolf,[6] and P. Adelmann[6]

[1]*Graduate Institute of Applied Physics and Department of Physics, National Taiwan University, Taipei 106, Taiwan*
[2]*Department of Physics, National Cheng Kung University, Tainan 70101, Taiwan*
[3]*Quantum Beam Science Directorate, Japan Atomic Energy Agency (JAEA), Tokai, Ibaraki 319-1195, Japan*
[4]*National Synchrotron Radiation Research Center, Hsinchu 30076, Taiwan*
[5]*Jülich Centre for Neutron Science (JCNS), Forschungszentrum Jülich GmBH, Outstation at FRM-II, Lichtenbergstrasse 1, D-85747 Garching, Germany*
[6]*Karlsruhe Institute of Technology (KIT), Institut fuer Festkoerperphysik, D-76021, Karlsruhe, Germany*

(Received 4 October 2010; revised manuscript received 2 February 2011; published 7 April 2011)

Longitudinal and Hall resistivities, scaling behavior, and magnetizations are examined to study the effect of flux pinning in $Ba(Fe_{1-x}Co_x)_2As_2$ (BFCA) single crystals with $x = 0.08$ and 0.01. Larger values of activation energy, critical current density, and pinning force are obtained in BFCA with $x = 0.10$, indicating relatively strong pinning. The sign reversal of Hall resistivities is clearly observed in BFCA with $x = 0.10$. The correlation between longitudinal and Hall resistivities shows the scaling behavior of $\rho_{xy} \propto (\rho_{xx})^{\beta}$ with exponents $\beta = 3.0$–3.4 and 2.0 ± 0.2 for BFCA crystals with $x = 0.08$ and 0.10, respectively. Furthermore, the normal-state Hall angle is also observed to follow $\cot \theta_H = \Lambda T^2 + C$ in BFCA crystals, and is explained by the Anderson theory. The relatively large C/Λ value for BFCA with $x = 0.10$ also implies a larger contribution of impurity scattering due to more Co atoms, which may cause stronger pinning of flux lines. The results are analyzed and coincide with theory, including the pinning-induced backflow effect and plastic flow mechanism in vortex dynamics.

DOI: 10.1103/PhysRevB.83.134506 PACS number(s): 74.25.F−, 74.25.Wx, 74.70.Xa

I. INTRODUCTION

Strong interest in transport properties has been stimulated by the discovery of superconductivity in FeAs-based compounds. In oxygen-free iron pnictides of RFe_2As_2 ($R = $ Ca, Sr, and Ba), hole doping by a potassium dopant has reached superconducting critical temperatures T_c of 38 K,[1–3] whereas electron doping by a cobalt dopant reveals superconductivity at temperatures below 22 K.[4] To date, transport-property studies have shown low anisotropy, weak thermal fluctuation, and high upper critical fields in RFe_2As_2 compounds.[5–7] Similar to high-T_c superconducting cuprates, iron-based pnictides reveal rich properties in the mixed state. For example, magnetization and relaxation measurements on $Ba(Fe_{1-x}Co_x)_2As_2$ (BFCA) compounds have shown a prominent second-peak effect, which is explained by a crossover from the collective to the plastic creep regime or a vortex structure phase transition from a rhombic to square lattice in the H-T phase diagram.[8–10] In contrast to BFCA compounds, however, $Ca(Fe_{1-x}Co_x)_2As_2$ crystals do not exhibit such a second peak in the field dependence of magnetization, corresponding to one possibility of only the plastic creep mechanism in vortex dynamics.[11] Meanwhile, a recent study with small-angle neutron scattering and magnetic force microscopy suggested that the vortices remain in the single-vortex pinning limit in fields up to 9 T, which is inconsistent with the prediction of the collective pinning model.[12] Obviously, there remain questions about the vortex dynamics in RFe_2As_2 compounds.

On the other hand, the anomalous Hall effect in the mixed state of type-II superconductors has been one of the most interesting subjects in the past two decades, and remains puzzling to researchers. In early works, transport measurements on certain high-T_c superconductors have shown an anomalous sign reversal of Hall resistivity,[13–18] which has been attributed to vortex pinning and vortex-vortex interaction,[19–21] or strong thermal fluctuation calculated in the time-dependent Ginzburg-Landau model.[22] Related theoretical works can be also found out in the references listed in Refs. 16 and 18. The experimental results have demonstrated that the sign reversal of Hall resistivity is not only a phenomenon near T_c, but a characteristic of the mixed state. Moreover, many researchers have argued that this effect should be viewed as a general consequence of vortex dynamics. The anomalous Hall effect is probably caused by flux pinning. For example, experimental results have shown a double sign reversal of Hall resistivity ρ_{xy} for $YBa_2Cu_3O_y$ (YBCO) films in the strong pinning limit,[15] or a diminishing sign reversal of ρ_{xy} for $YBa_2Cu_3O_y/PrBa_2Cu_3O_y$ (YBCO/PBCO) superlattices with weaker pinning.[18] This is a topic of current interest but has never been examined in the new superconducting FeAs-based families.[23] Previous research has investigated Hall measurements on iron-based pnictides for their transport properties in a normal state.[4,24–28] In this work, we study the mixed-state transport properties of BFCA single crystals with $x = 0.08$ and 0.10. We present a systematic investigation of the correlation between Hall resistivities and flux pinning in BFCA single crystals. Here the issue of flux pinning in BFCA with different Co dopants is interesting and worth debate since the overdoped Co contents seem to increase the number of pinning centers but accompany them with a lower T_c.[9] Little is known about the role of Co contents in flux pinning. We will begin with the electrical-transport and magnetization measurements to probe the flux-pinning strength and mechanism in BFCA single crystals. Then we present the measured Hall resistivities and their scaling behavior correlated to longitudinal resistivities

and show a sign reversal of the mixed-state Hall coefficient and stronger flux pinning for the BFCA single crystal with $x = 0.10$, which is the most interesting result in this article. The origin of stronger pinning in BFCA with $x = 0.10$ is debated via the analyses of the normal-state Hall angle. Finally we quantitatively analyze the sign reversal of Hall resistivity and the pinning force for BFCA with $x = 0.10$. All results are discussed in terms of the existing theories.

II. EXPERIMENTAL

BFCA single crystals were grown from self-flux in an alumina crucible and the crystals grown with the same batch show very similar properties, as described previously.[29] The crystals were well-formed plates and characterized by an x-ray diffractometer using Cu $K\alpha$ radiation. The compositions have been determined by means of energy-dispersive x-ray spectroscopy done at different sites of each sample, and show a homogeneous Co distribution. For transport measurements, the crystals were cut into dimensions of $3\times1.5\times0.03$ mm^3. The crystal a axis, which was determined by Laue x-ray diffraction, is almost parallel to the longest axis. Five leads were soldered with indium, and a Hall-measurement geometry was constructed to allow simultaneous measurements of both longitudinal (ρ_{xx}) and transverse (Hall) resistivities (ρ_{xy}) using standard dc techniques. Hall voltages were taken in opposing fields parallel to the c axis up to 7 T and at a dc current density of $\sim$50 A/cm^2. The magnetization was measured in a superconducting quantum interference device (SQUID) system (MPMS from Quantum Design).

III. RESULTS AND DISCUSSION

Figure 1 shows the x-ray θ-2θ diffraction spectrum for BFCA with $x = 0.10$, in which only the (00n) ($n = 2$, 4, 6, 8, and 10) diffraction peaks were observed, indicating that the [001] direction is perpendicular to the plane of the crystals. The inset of Fig. 1 shows the x-ray θ-2θ diffraction spectra in the region near the (008) peak for BFCA samples with $x = 0.08$ and 0.10. The peaks are broad and have a shoulder at

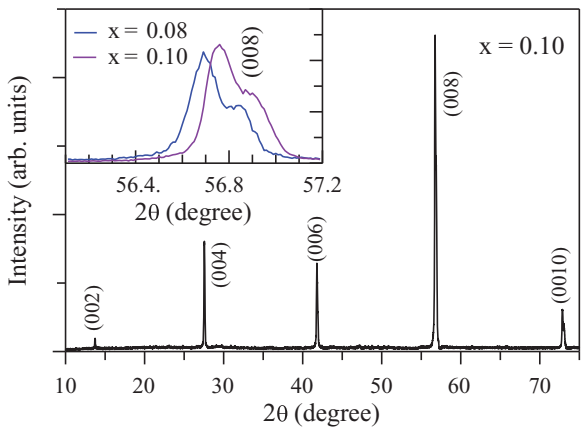

FIG. 1. (Color online) X-ray θ-2θ diffraction spectrum for BFCA with $x = 0.10$. The inset shows the x-ray θ-2θ diffraction spectra in the region near the (008) peak for BFCA samples with $x = 0.08$ and 0.10.

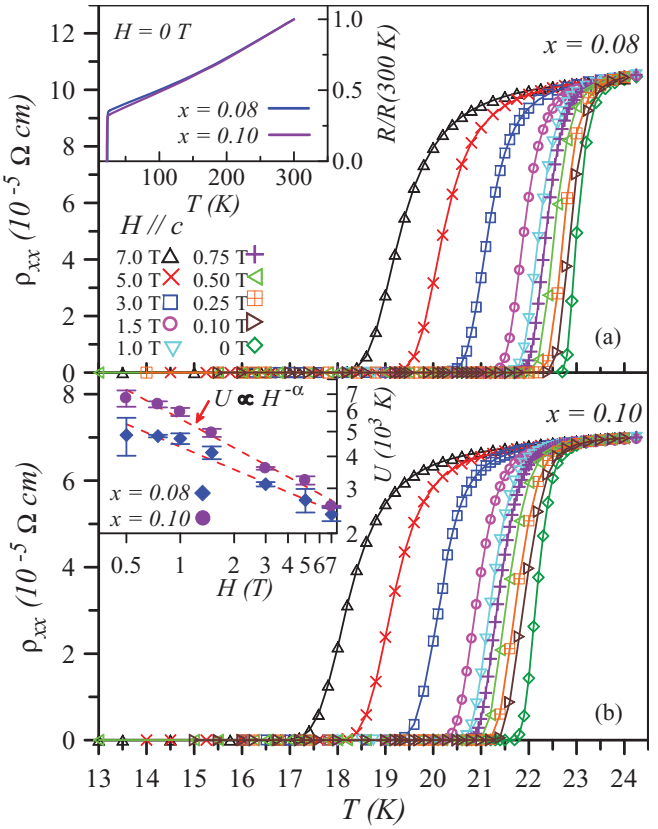

FIG. 2. (Color online) Resistivity as a function of temperature with magnetic fields parallel to the crystal c axis for BFCA samples (a) with $x = 0.08$ and (b) 0.10. Inset of (a): Temperature-dependent resistances normalized to their room-temperature values in zero field. Inset of (b): Field-dependent activation energy for BFCA crystals with $x = 0.08$ and 0.10. The dashed lines indicate the fitting of $U \propto H^{-\alpha}$.

a higher 2θ angle due to the Cu $K\alpha_1$ and Cu $K\alpha_2$ radiations. As can be seen, the (008) peak for BFCA with $x = 0.10$ positions at a higher angle due to a small decrease in the length of the c axis. The lattice constants of the c axis can be determined precisely to be 12.979 and 12.964 Å for BFCA samples with $x = 0.08$ and 0.10, respectively. The values of the lattice constant are very close to those of BFCA samples with the same compositions reported by Ni *et al.*[30] This result is in agreement with the elemental analysis of their samples performed using wavelength-dispersive x-ray spectroscopy.

Hall coefficient and electrical resistivities in the presence of magnetic fields for BFCA crystals in the mixed state were systematically investigated. Figures 2(a) and 2(b) show the resistivity as a function of temperature in magnetic fields parallel to the crystal c axis for BFCA samples with $x = 0.08$ and 0.10, respectively. The inset of Fig. 2(a) shows the temperature-dependent resistances normalized to their room-temperature values in zero field for BFCA samples within a wide temperature region. As seen, both the normal-state resistances for samples show metallic behavior, varying roughly linearly with temperature. The superconducting critical temperatures T_c, defined by extrapolating the zero-field resistive transition to $\rho_{xx} = 0$, are 22.7 and 21.8 K for BFCA samples with $x = 0.08$ and 0.10, respectively. The data are

similar to those previously reported.[4–6] In Figs. 2(a) and 2(b), the resistivity under magnetic field shows a broadening behavior due to thermally activated flux motion, which has been proposed by Anderson and Kim,[31,32] and can be described by

$$\rho_{xx}(T,H) = \rho_0 \exp(-U/k_B T). \quad (1)$$

Here U is the activation energy, which is normally both field and temperature dependent. The inset of Fig. 2(b) shows the field-dependent activation energy extracted from Eq. (1) via the Arrhenius plots for BFCA crystals with $x = 0.08$ and 0.10. In the Anderson-Kim model, the activation energy U is an indication of the magnitude of effective pinning energy. As seen in the inset, the activation energies for BFCA with $x = 0.10$ are larger than those for BFCA with $x = 0.08$, and the values of U for BFCA are approximately one order of magnitude smaller than those of several 10^4 K for YBCO,[33] indicating a relatively weak vortex pinning in BFCA. The values of U obtained in this study are larger than the reported data[8,9] deduced from the magnetization relaxation rate. Such a difference is due to the relatively very low current density applied in our transport measurements. As seen in the inset of Fig. 2(b), U can be fitted with an approximate field dependence of $U \propto H^{-\alpha}$ with $\alpha = 0.29$ and 0.38 for BFCA crystals with $x = 0.08$ and 0.10, respectively. The present observation of thermally activated behavior for BFCA in a mixed state is similar to those of $\alpha = 0.33$–0.88 observed on high-T_c superconducting cuprates, as mentioned in Ref. 33. The power-law dependence of U with $\alpha = 0.5$ has been proposed for YBCO crystals within the plastic vortex creep model.[34] Obviously, the activation energy does not scale with the predicted H^{-1} dependence[35] or the $H^{-0.5}$ dependence. A slight deviation of α from a value of 0.5 for BFCA crystals possibly results from the crossover in flux dynamics from elastic to plastic creep as seen in YBCO crystals.[34] A much slower field dependence of U with $U \propto H^{-0.13}$ has been reported recently on $Ba_{0.72}K_{0.28}Fe_2As_2$ single crystals.[36] The origin of this deviation requires further study.

Figure 3(a) shows two typical magnetization hysteresis loops measured at a temperature of $0.8T_c$ for BFCA crystals with $x = 0.08$ and 0.10 in fields parallel to the c axis. According to the Bean critical state model,[37] the superconducting critical current density J_c can be calculated. The inset of Fig. 3(a) shows J_c versus the reduced temperature T/T_c in zero field and 1 T for the corresponding samples. In Fig. 3(b), the field dependences of J_c at 0.8 and $0.9T_c$ are presented. As can be seen, the BFCA crystal with $x = 0.10$ exhibits a larger critical current density at temperatures near T_c, which is in agreement with the stronger pinning observed on the thermally activated flux motion in it. Furthermore, the second magnetization peak, which indicates the fishtail effect, can be clearly observed in the BFCA crystal with $x = 0.10$, as seen in Fig. 3(a). As mentioned previously, different scenarios have been proposed to account for the origin of the observed second magnetization peak.[8–12] However, regardless of which scenario is adopted, be it a change in the dynamics of the vortex[10] or a transition from the collective pinning to plastic pinning,[8,9] the appearance of the second magnetization peak implies relatively strong pinning in BFCA with $x = 0.10$, which is consistent with the

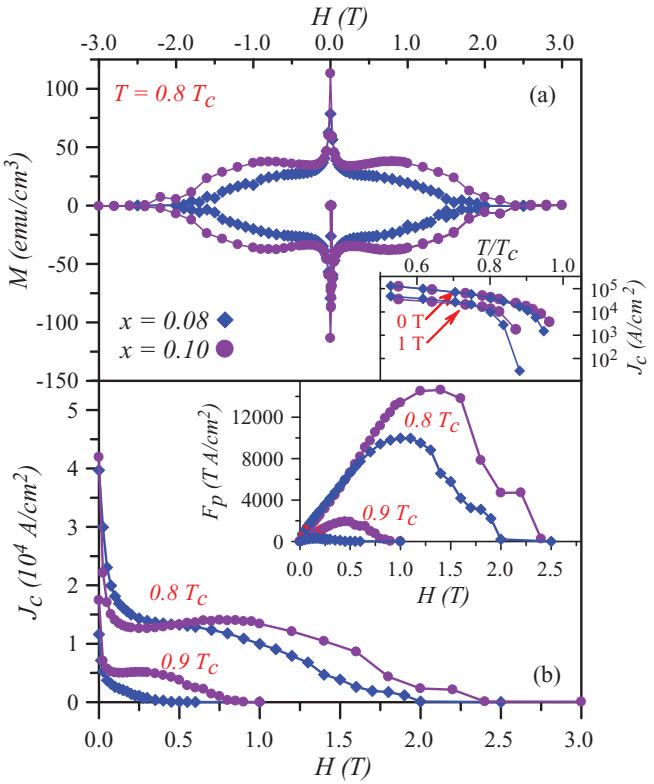

FIG. 3. (Color online) (a) Magnetization hysteresis loops measured at $0.8T_c$ for BFCA crystals with $x = 0.08$ and 0.10 in fields parallel to the c axis. (b) Field dependences of critical current density J_c at 0.8 and $0.9T_c$ for the corresponding samples. Inset of (a) shows J_c versus the reduced temperature T/T_c in zero field and 1 T for the corresponding samples. Inset of (b) shows the corresponding pinning forces against the magnetic field.

obtained larger values of activation energy and critical current density. The inset of Fig. 3(b) shows the corresponding pinning forces against the magnetic field, which were obtained from J_c as $F_p = H J_c$. At temperature $0.8T_c$, the maximum pinning force occurs at the field H_{mp} of 1.4 (1.0) T, and the pinning force extrapolates to zero at the field H_{0p} of 2.4 (2.0) T for BFCA with $x = 0.10$ (0.08). For the maximum reduced field h_m, defined as $h_m = H_{mp}/H_{0p}$, we obtain $h_m = 0.50$ and 0.58 for BFCA with $x = 0.08$ and 0.10, respectively. The obtained values of h_m are slightly larger than those of 0.37 and 0.45 obtained in BFCA crystals with $x = 0.075$ and 0.10 by Sun *et al.*[6] and Yamamoto *et al.*,[7] respectively. This is an interesting subject that should be treated much more adequately elsewhere. The parameters of activation energy, maximum pinning force at $0.8T_c$, α, and h_m for BFCA with $x = 0.08$ and 0.10 are listed in Table I for comparison. Indeed, stronger pinning was observed on the BFCA with the $x = 0.10$ sample. In addition, one can see that the values of activation energy in a field 1 T, $U(1\ \mathrm{T})$, for our BFCA samples are comparable with that of ~5000 K for $Ba_{0.72}K_{0.28}Fe_2As_2$ single crystals.[36] Other parameters also shown in Table I will be discussed later.

Figures 4(a) and 4(b) show the temperature dependence of Hall resistivity ρ_{xy} for BFCA samples with $x = 0.08$ and 0.10, respectively. The negative normal-state Hall resistivity ρ_{xy} reveals an electron-dominating transport, and gradually becomes

TABLE I. Values of activation energy U in a field of 1 T and maximum pinning force $F_{p,\max}$ at $0.8T_c$ for BFCA with $x = 0.08$ and 0.10. Also shown are the derived parameters of exponent α, maximum reduced field h_m, exponent β, and C/Λ as described in the text. Some parameters for $Ba_{0.72}K_{0.28}Fe_2As_2$ single crystals are also shown for comparison.

Samples	U(1 T) (K)	$F_{p,\max}$ (T A/cm^2)	α	h_m	β	C/Λ (K^2)
BFCA						
$x = 0.08$	4693 ± 226	9959	0.29	0.50	3.0–3.4	16 107
$x = 0.10$	5965 ± 216	14 618	0.38	0.58	2.0 ± 0.2	19 623
$Ba_{0.72}K_{0.28}Fe_2As_2$ (Ref. 36)	~5000	—	0.13	—	—	—

zero with decrease in temperature. The most interesting is the sign reversal of ρ_{xy} observed on the sample of BFCA with $x = 0.10$, while the Hall resistivity ρ_{xy} of BFCA with $x = 0.08$ does not go into a sign reversal in the mixed state. The inset of Fig. 4(a) shows the Hall coefficient versus temperature for BFCA with $x = 0.10$. The sign reversal of the Hall coefficient can be more clearly observed. One can see that the maximum positive Hall coefficient depends on the magnetic field, and show a concave downward behavior. Figure 4(c) shows the temperature dependence of Hall resistivity ρ_{xy} taken on the other two samples with $x = 0.08(S'_{0.08})$ and $0.10(S'_{0.10})$ in fields of 1.0 and 1.5 T. The two samples are respectively from the same batches for samples previously studied, and individually reveal similar temperature dependences to those as seen in Figs. 4(a) and 4(b). Again, the sign reversal of ρ_{xy} is observed on the $S'_{0.10}$ sample, while the Hall resistivity ρ_{xy} of $S'_{0.08}$ does not go into a sign reversal in the mixed state. The inset of Fig. 4(c) shows the resistive transition for $S'_{0.10}$ and $S'_{0.08}$ samples. The superconducting critical temperatures are 22.5 and 21.9 K for $S'_{0.10}$ and $S'_{0.08}$ samples, respectively. The activation energy U(1 T) of 6105 ± 66 K for $S'_{0.10}$ is larger than that of 4563 ± 92 K for the $S'_{0.08}$ sample. All the transport properties are very similar to those previously observed. In the following we shall confine our attention to the properties for the two typical samples as seen in Figs. 4(a) and 4(b).

Additionally, for a fixed temperature, the magnetic-field dependence of ρ_{xy} was also studied. Figures 5(a) and 5(b) show the magnetic-field dependence of ρ_{xy} for BFCA with $x = 0.08$ and 0.10 at various temperatures, respectively. As can be seen, the Hall resistivity of BFCA with $x = 0.08$ does not reveal an anomalous sign reversal in the measured-temperature region, while the sign reversal of Hall resistivity can be observed on BFCA with $x = 0.10$ at the measured temperatures, which is consistent with the results shown in Figs. 4(a) and 4(b). As seen in Fig. 5(b), the magnitude of positive maximum Hall resistivity, $\rho_{xy,\max}$, increases with an increase in temperature, reaching a maximum at 21.0 K, and then diminishes with a further increase in temperature. The observed sign-reversal behavior of Hall resistivity for BFCA in the mixed state is similar to those observed on high-T_c superconducting cuprates and MgB_2 films.[38] Besides the anomalous sign reversal of Hall resistivity, another interesting feature in the mixed-state Hall effect is the scaling behavior, $\rho_{xy} \propto (\rho_{xx})^{\beta}$. The insets of Fig. 5(a) and 5(b) demonstrate the plots of $\log_{10}|\rho_{xy}|$ vs $\log_{10}\rho_{xx}$ for BFCA with $x = 0.08$ and 0.10, respectively. The data were taken respectively at fixed magnetic fields and fixed temperatures shown in Figs. 4 and 5, respectively. In the inset of Fig. 5(a), the data for BFCA with $x = 0.08$ clearly display the power-law relationship encompassing a variation in ρ_{xy} of three orders of magnitude from the detected limit of $\sim 10^{-10}$ Ω cm. The data taken from the fixed-magnetic-field and fixed-temperature measurements follow the power-law relationship with $\beta = 3.0 \pm 0.1$ and 3.4 ± 0.4, respectively. In the inset of Fig. 5(b), the data for BFCA with $x = 0.10$ also follow the scaling correlation with $\beta = 2.0 \pm 0.2$ in the regime of positive Hall resistivity. The cusp in the inset of Fig. 5(b) is an artifact of the absolute value $|\rho_{xy}|$, corresponding to where ρ_{xy} passes through zero. This scaling law was first observed by Luo *et al.*[39] for YBCO films with $\beta = 1.7 \pm 0.2$ and by Samoilov *et al.*[40] for $Bi_2Sr_2CaCu_2O_y$ single crystals with $\beta = 2.0 \pm 0.1$. The Hall scaling behavior is a complicated phenomena, and a number of theories have been proposed to account for it. Dorsey and Fisher[41] developed a scaling theory in terms of glassy scaling near the vortex-glass transition and obtained an appropriate value $\beta = 1.7$. An alternative model where $\beta = 2.0$ in the thermally assisted flux-flow region was suggested by Vinokur *et al.*[42] Wang, Dong, and Ting (WDT)[19] also developed a unified theory for the anomalous Hall effect including both the flux pinning effect and thermal fluctuations. They explained the sign reversal of Hall resistivity and scaling behavior by taking into account the backflow current effect on flux motion due to pinning, and achieved the scaling exponent β changing from 2 to 1.5 for increasing pinning. Many studies[13,43,44] on high-T_c superconductors with columnar defects adopted WDT's theory to describe their experimental results. Other proposed theories, such as the calculation of σ_{xy} for d-wave superconductors having $\beta = 1$,[45] and the idea[46] of β varying from 1.4 to 2.0 during the dimensional crossover from a three-dimensional to a two-dimensional vortex state as the magnetic field increases have also been presented. Here the exponent $\beta = 2.0 \pm 0.2$ for BFCA with $x = 0.10$ is in agreement with the results in theories or experiments on high-T_c superconductors. However, the exponent $\beta = 3.0-3.4$ for BFCA with $x = 0.08$ seems to be beyond the theoretical prediction. Considering WDT's theory, a larger β value implies weaker pinning, which is consistent with the relatively low activation energy, critical current density, and pinning force for BFCA with $x = 0.08$ as previously presented, and results in a diminishing sign reversal of ρ_{xy} in mixed state. Larger β values exceeding 2 have also been observed on YBCO/PBCO superlattices with weaker pinning.[18] More theoretical details on the pinning dependence of the β value are necessary.

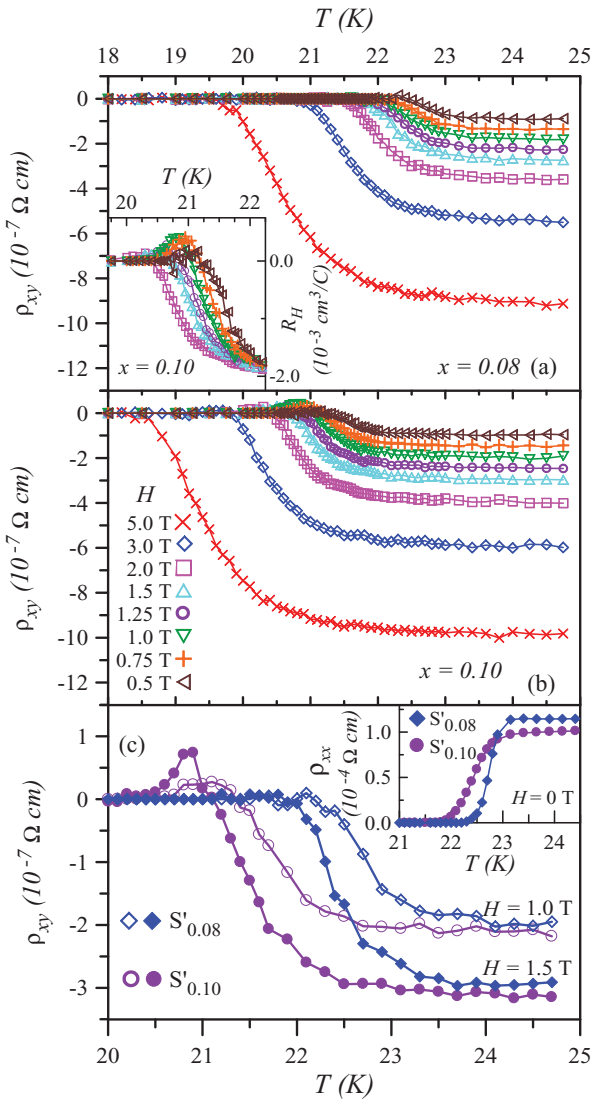

FIG. 4. (Color online) Temperature dependence of ρ_{xy} for BFCA samples with (a) $x = 0.08$ and (b) 0.10. Inset of (a): Hall coefficient versus temperature for BFCA with $x = 0.10$. (c) Temperature dependence of Hall resistivity ρ_{xy} taken on the other two samples as described in the text. Inset of (c): Resistive transition for the corresponding samples.

The relatively strong pinning in BFCA with $x = 0.10$, as we have noted before, is an interesting subject and needs to be further examined. Pinning generally originates from the pointlike impurities, defects (vacancies), or twin structure and magnetic domain boundaries in single-crystal superconductors, which will exhibit their characteristic transport properties in normal state. Anderson[47] has proposed a clue to perceive the normal-state Hall anomaly by distinguishing between the relaxation rates for the carrier motion normal to the Fermi surface and parallel to it. The theory predicts especially the behavior of the Hall angle when in-plane impurities are introduced and has been applied to high-T_c superconductors.[48–50] According to Anderson's theory,[47] the transverse (Hall) relaxation rate is determined by scattering between excitations, and varies with T^2. The scattering from magnetically active impurities introduces additional terms in the transport scattering rate $1/\tau_{tr}$

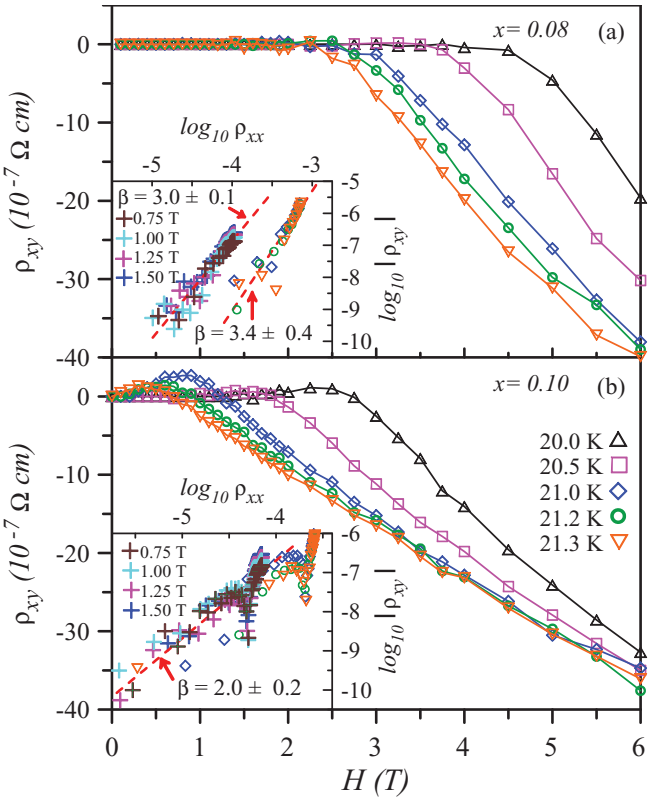

FIG. 5. (Color online) Magnetic-field dependence of ρ_{xy} for BFCA with (a) $x = 0.08$ and (b) 0.10 at various temperatures. Insets of (a) and (b) demonstrate the plots of $\log_{10}|\rho_{xy}|$ vs $\log_{10}\rho_{xx}$ taken respectively at fixed magnetic fields and fixed temperatures for the corresponding samples. The dashed lines indicate the fitting of $\rho_{xy} \propto (\rho_{xx})^{\beta}$.

and Hall relaxation rate $1/\tau_H$. For the transverse scattering rate, Anderson introduced

$$1/\tau_H = T^2/J + 1/\tau_M, \tag{2}$$

where J is the bandwidth of spin excitations (or the spin-exchange energy in Anderson's theory) and $1/\tau_M$ is the impurity contribution. For the Fermi surface formed by spinons, the transport scattering rate $1/\tau_{tr}$ is proportional to the resistivity, i.e., σ_{xx}, which is, in turn, proportional to τ_{tr}, whereas σ_{xy} is proportional to $\tau_H \tau_{tr}$. On the other hand, the Hall angle $\theta_H = \tan^{-1}(\sigma_{xy}/\sigma_{xx})$ involves $1/\tau_H$ only, and Eq. (2) implies

$$\cot\theta_H = 1/(\omega_c \tau_H) = \Lambda T^2 + C, \tag{3}$$

where $\omega_c = eB/m^*$, m^* is an effective mass, and C is the impurity contribution. Combining Eqs. (2) and (3), we can see that Λ corresponds to $1/(J\omega_c)$ and $C = 1/(\tau_M \omega_c)$. The value of $C/\Lambda = J(1/\tau_M)$, which is independent of the effective spinon mass, can reflect the product of spin-exchange energy and impurity scattering rate.

To verify Eq. (3), in Fig. 6(a) we have plotted $\cot\theta_H$ vs T^2 for BFCA with $x = 0.08$ and 0.10 measured in a field of 7 T. As can be seen, the data fall on a straight line in the temperature range below ~245 K. By using the line fitted to Eq. (3), the parameters Λ and C can be obtained. For BFCA with $x = 0.08$, the values of Λ and C are 4.84 mK^{-2} and 78.04,

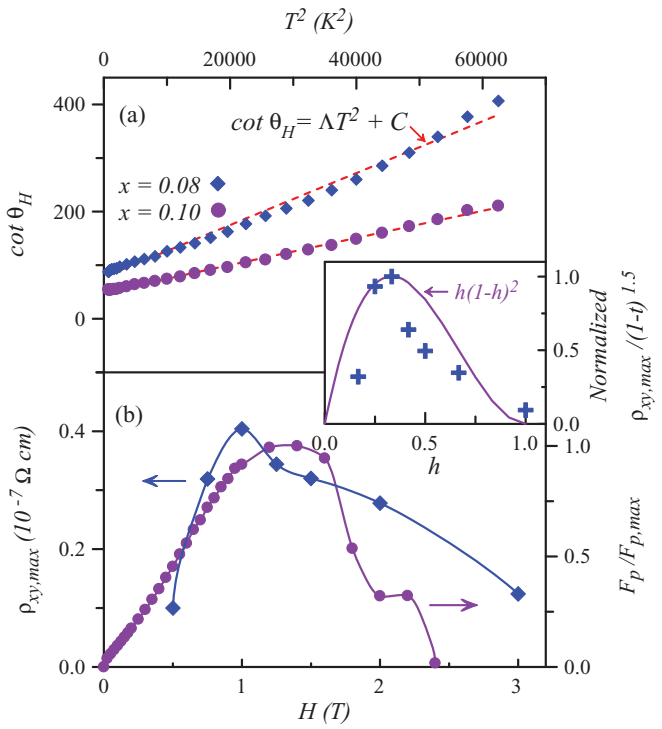

FIG. 6. (Color online) (a) Temperature dependence of the Hall angle shown as cot θ_H vs T^2 for BFCA with $x = 0.08$ and 0.10 measured in field of 7 T. The dashed lines indicate the fitting of cot $\theta_H = \Lambda T^2 + C$. (b) $\rho_{xy,\max}$ extracted at different fields and field dependence of normalized pinning force $F_p/F_{p,\max}$ for BFCA with $x = 0.10$ at $0.8T_c$. Inset : Normalized $\rho_{xy,\max}/(1-t)^{1.5}$ against the reduced field h. Also shown in the inset is a normalized $h(1-h)^2$ curve for comparison.

respectively, whereas the values of Λ and C are 2.53 mK^{-2} and 49.62, respectively for BFCA with $x = 0.10$. Therefore, the values of C/Λ are 16107 and 19623 K^2 for BFCA with $x = 0.08$ and 0.10, respectively. If Co doping has little effect on J, as reported on the $La_{1.85}Sr_{0.15}Cu_{1-x}A_xO_4$ (A = Fe, Co, Ni, Zn, Ga) systems,[49] the relatively large C/Λ value for BFCA with $x = 0.10$ infers a larger contribution of impurity scattering to the transport in normal state. This impurity scattering, due to more Co atoms in the FeAs plane, may cause the pinning of flux lines by pointlike defects, disorder, or twin structure and magnetic domain boundaries when the temperature decreases into the mixed state. It should be noted that the presence of such disorder is not necessarily an issue of sample quality, as pointed by Inosov *et al.*[12] for their BFCA single crystals. Moreover, it is worthwhile to point out that Rullier-Albenque *et al.*[25] have recently obtained the same results of T^2 dependence of cot θ_H for their BFCA samples and described this behavior by considering the electron-electron scattering. Both the spinon-spinon scattering and fermion-fermion interaction can lead to the T^2 process. Thus, the normal-state transport mechanism merits more in-depth investigation. The values of the obtained exponent β and C/Λ for BFCA samples are also shown in Table I for comparison. A smaller β value and a larger C/Λ ratio suggest a scenario of stronger pinning originated from more impurity scattering for BFCA with $x = 0.10$. It is interesting that even though the T_c is slightly lower than that of the optimally doped sample, the flux pinning can be enhanced by adding the Co dopant in BFCA. However, as reported by Shen *et al.*,[9] for an overdoped sample with $x = 0.12$, the pinning energy falls down to be much smaller than that of the optimally doped sample. A full understanding of the likely competition between strengthening of superconductivity by doping and weakening by disorder and/or impurities needs more samples with different compositions studied. Our electrical and magnetization measurements provide a significant understanding to the flux pinning in BFCA with $x = 0.10$, which shows Hall sign reversal in mixed state.

Having observed the sign reversal of Hall resistivity and noticing relatively strong pinning in BFCA with $x = 0.10$, one can then proceed to consider WDT's theory for describing the anomalous mixed-state Hall effect. In an earlier paper,[51] Wang and Ting have approximated the behavior of the maximum Hall resistivity $\rho_{xy,\max}$ in the sign reversal region as described by

$$\rho_{xy,\max} \approx \frac{|F_p|}{J_T}\frac{1}{Ne}, \tag{4}$$

where F_p is the average pinning force, J_T is the transport current density, and N is the carrier concentration.

The magnitude of $\rho_{xy,\max}$ being proportional to the average pinning force is the most important consequence of Wang and Ting's theory. From Eq. (4), an appropriate form of F_p can be obtained to approximate the variation of $\rho_{xy,\max}$ with different fields or temperatures. Since the transport current in our measurements is constant, the magnitude of $\rho_{xy,\max}$ is only proportional to the average pinning force. If the temperature dependence and magnetic-field dependence of F_p can be determined, the behavior of $\rho_{xy,\max}$ can be understood by Wang and Ting's theory. Figure 6(b) shows the $\rho_{xy,\max}$ extracted at different fields. For comparison, the field dependence of normalized pinning force $F_p/F_{p,\max}$ for BFCA with $x = 0.10$ at temperature of $0.8T_c$ is also shown in Fig. 6(b). As can be seen, the variations of both $\rho_{xy,\max}$ and $F_p/F_{p,\max}$ show a concave downward behavior. Since $\rho_{xy,\max}(H)$ occurs at different temperatures while F_p is obtained at fixed temperatures, the temperature dependence of $\rho_{xy,\max}$ should be taken into account. Nishizaki *et al.*[52] have proposed that the temperature dependence of F_p is proportional to $(1-t)^{1.5}$ near T_c, where t stands for the reduced temperature. After substituting the proportion factor $(1-t)^{1.5}$ into Eq. (4), the term $\rho_{xy,\max}/(1-t)^{1.5}$ should be independent of temperature. The inset of Fig. 6 plots the normalized $\rho_{xy,\max}/(1-t)^{1.5}$ against the reduced field h, which is defined by $h = H/H_0$ with $H_0 = 3$ T for the magnitude of $\rho_{xy,\max}$ falling down to near zero. Also shown in the inset of Fig. 6 is a normalized $h(1-h)^2$ curve for comparison. As can be seen, the magnitude of $\rho_{xy,\max}/(1-t)^{1.5}$ indeed shows a $h(1-h)^2$-like dependence, which is analogous to the point defect pinning as reported by Sun, Liu and Lin.[6] Here we also note the different field-dependence types between the normalized $\rho_{xy,\max}/(1-t)^{1.5}$ and $F_p/F_{p,\max}$ derived from our magnetization measurements. It is because they are obtained in different temperature regimes in which the vortex motion can be dominated by different types of pinning due to dimensional crossover.[53] In fact, the observed maximum positive Hall resistivities $\rho_{xy,\max}$ occur at the temperatures of 0.91–0.97t, which are higher than

those for the measured F_p. Our results are also in agreement with the calculation made by Zhu *et al.*[21] They expanded upon WDT's theory and showed that the boundaries of the sign-reversal ρ_{xy} region are located at temperatures near $0.97t$, which are close to the boundaries between the plastic flow liquid and elastic moving glass. The observed sign reversal of the mixed-state Hall resistivity coincides with the theory including the pinning-induced backflow effect and plastic flow mechanism in vortex dynamics.

IV. SUMMARY

In summary, the longitudinal and Hall resistivities, and the magnetizations of BFCA crystals with $x = 0.08$ and 0.01 are reported. For BFCA with $x = 0.10$, larger values of activation energy, critical current density, and pinning force are obtained, indicating relatively strong pinning. Also shown is the sign reversal of Hall resistivity evidently observed on BFCA with $x = 0.10$. Both samples show a scaling behavior of $\rho_{xy} \propto (\rho_{xx})^{\beta}$, where the exponent $\beta = 2.0 \pm 0.2$ for BFCA with $x = 0.10$ is in agreement with the theoretical and experimental results on high-T_c superconductors, and the exponent $\beta = 3.0$–3.4 for BFCA with $x = 0.08$ is beyond the theoretical prediction. Moreover, the normal-state Hall angle is also observed to follow $\cot \theta_H = \Lambda T^2 + C$ in BFCA crystals, and can be explained by the spinon-spinon scattering theory. The relatively large C/Λ value for BFCA with $x = 0.10$ implies a larger contribution of impurity scattering due to more Co atoms in the FeAs plane, which may cause stronger pinning of flux lines. Finally, Wang and Ting's theory is utilized to quantitatively analyze the observed sign reversal of Hall resistivity of BFCA with $x = 0.10$, and the variations of both $\rho_{xy,\max}$ and $F_p/F_{p,\max}$ in fields show an analogous behavior. The results coincide with the theory including the pinning-induced backflow effect and plastic flow mechanism in vortex dynamics.

ACKNOWLEDGMENTS

The authors thank the National Science Council of Taiwan for financial support under Grants No. NSC 98-2112-M-212-001-MY3 (L.M.W.), No. NSC 96-2739-M-213-001, and No. NSC 96-2112-M-007-012 (L.J.C.). T. W. and P. A. acknowledge financial support through the Deutsche Forschungsgemeinschaft (SPP 1458).

*liminwang@ntu.edu.tw
†hcyang@phys.ntu.edu.tw

[1] M. Rotter, M. Tegel, and D. Johrendt, Phys. Rev. Lett. **101**, 107006 (2008).
[2] K. Sasmal, B. Lv, B. Lorenz, A. M. Guloy, F. Chen, Y.-Y. Xue, and C.-W. Chu, Phys. Rev. Lett. **101**, 107007 (2008).
[3] N. Ni, S. L. Bud'ko, A. Kreyssig, S. Nandi, G. E. Rustan, A. I. Goldman, S. Gupta, J. D. Crobett, A. Kracher, and P. C. Canfield, Phys. Rev. B **78**, 014507 (2008).
[4] Athena S. Sefat, Rongying Jin, Michael A. McGuire, Brian C. Sales, David J. Singh, and David Mandrus, Phys. Rev. Lett. **101**, 117004 (2008).
[5] M. A. Tanater, N. Ni, C. Martin, R. T. Gordon, H. Kim, V. G. Kogan, G. D. Samolyuk, S. L. Bud'ko, P. C. Canfield, and R. Prozorov, Phys. Rev. B **79**, 094507 (2009).
[6] D. L. Sun, Y. Kiu, and C. T. Lin, Phys. Rev. B **80**, 144515 (2009).
[7] A. Yamamoto, J. Jaroszynski, C. Tarantini, L. Balicas, J. Jiang, A. Gurevich, D. C. Larbalestier, R. Jin, A. S. Sefat, M. A. McGuire, B. C. Sales, D. K. Christen, and D. Mandrus, Appl. Phys. Lett. **94**, 062511 (2009).
[8] R. Prozorov, N. Ni, M. A. Tanatar, V. G. Kogan, R. T. Gordon, C. Martin, E. C. Blomberg, P. Prommapan, J. Q. Yan, S. L. Bud'ko, and P. C. Canfield, Phys. Rev. B **78**, 224506 (2008).
[9] Bing Shen, Peng Cheng, Zhaosheng Wang, Lei Fang, Cong Ren, Lei Shan, and Hai-Hu Wen, Phys. Rev. B **81**, 014503 (2010).
[10] R. Kopeliansky, A. Shaulov, B. Ya. Shapiro, Y. Yeshurun, B. Rosenstein, J. J. Tu, L. J. Li, G. H. Cao, and Z. A. Xu, Phys. Rev. B **81**, 092504 (2010).
[11] A. K. Pramanik, L. Harnagea, S. Singh, S. Aswartham, G. Behr, S. Wurmehl, C. Hess, R. Klingeler, and B. Buchner, Phys. Rev. B **82**, 014503 (2010).
[12] D. S. Inosov, T. Shapoval, V. Neu, U. Wolff, J. S. White, S. Haindl, J. T. Park, D. L. Sun, C. T. Lin, E. M. Forgan, M. S. Viazovska, J. H. Kim, M. Laver, K. Nenkov, O. Khvostikova, S. Kuhnemann, and V. Hinkov, Phys. Rev. B **81**, 014513 (2010).
[13] W. N. Kang, D. H. Kim, S. Y. Shim, J. H. Park, T. S. Hahn, S. S. Choi, W. C. Lee, J. D. Hettinger, K. E. Gray, and B. Glagola, Phys. Rev. Lett. **76**, 2993 (1996)
[14] W. N. Kang, B. W. Kang, Q. Y. Chen, J. Z. Wu, Y. Bai, W. K. Chu, D. K. Christen, R. Kerchner, and Sung-Ik Lee, Phys. Rev. B **61**, 722 (2000).
[15] W. Gob, W. Liebich, W. Lang, I. Puica, Roman Sobolewski, R. Rossler, J. D. Pedarnig, and D. Bauerle, Phys. Rev. B **62**, 9780 (2000).
[16] I. Puica, W. Lang, W. Gob, and R. Sobolewski, Phys. Rev. B **69**, 104513 (2004).
[17] H. Richter, I. Puica, W. Lang, M. Peruzzi, J. H. Durrell, H. Sturm, J. D. Pedarnig, and D. Bauerle, Phys. Rev. B **73**, 184506 (2006).
[18] L. M. Wang, H. C. Yang, and H. E. Horng, Phys. Rev. Lett. **78**, 527 (1997).
[19] Z. D. Wang, Jinming Dong, and C. S. Ting, Phys. Rev. Lett. **72**, 3875 (1994).
[20] P. Ao, Condens. Matter **10**, L677 (1998)
[21] B. Y. Zhu, D. Y. Xing, Z. D. Wang, B. R. Zhao, and Z. X. Zhao, Phys. Rev. B **60**, 3080 (1999).
[22] Robert J. Troy and Alan T. Dorsey, Phys. Rev. B **47**, 2715 (1993)
[23] Hechang Lei, Rongwei Hu, E.S. Choi, and C. Petrovic, Phys. Rev. B **82**, 134525 (2010); After the manuscript was submitted, Lei *et al.*, reported on the mixed-state Hall effect of Fe(Te,S) single crystals. They showed the thermally activated energies which are smaller than 200 K, and did not observe the Hall sign reversal.
[24] G. F. Chen, Z. Li, J. Dong, G. Li, W. Z. Hu, X. D. Zhang, X. H. Song, P. Zheng, N. L. Wang, and J. L. Luo, Phys. Rev. B **78**, 224512 (2008).

[25]F. Rullier-Albenque, D. Colson, A. Forget, and H. Alloul, Phys. Rev. Lett. **103**, 057001 (2009).
[26]Lei Fang, Huiqian Luo, Peng Cheng, Zhaosheng Wang, Ying Jia, Gang Mu, Bing Shen, I. I. Mazin, Lei Shan, Cong Ren, and Hai-Hu Wen, Phys. Rev. B **80**, 140508 (2009).
[27]Eun Deok Mun, Sergey L. Bud'ko, Ni Ni, Alex N. Thaler, and Paul C. Canfield, Phys. Rev. B **80**, 054517 (2009).
[28]I. Tsukada, M. Hanawa, Seiki Komiya, T. Akiike, R. Tanaka, Y. Imai, and A. Maeda, Phys. Rev. B **81**, 054515 (2010).
[29]Frédéric Hardy, Peter Adelmann, Thomas Wolf, Hilbert v. Löhneysen, and Christoph Meingast, Phys. Rev. Lett. **102**, 187004 (2009).
[30]N. Ni, M. E. Tillman, J.-Q. Yan, A. Kracher, S. T. Hannahs, S. L. Bud'ko, and P. C. Canfield, Phys. Rev. B **78**, 214515 (2008).
[31]P. W. Anderson, Phys. Rev. Lett. **9**, 309 (1962).
[32]Y. B. Kim, C. F. Hempstead, and A. R. Strnad, Phys. Rev. **131**, 2486 (1963).
[33]H. C. Yang, L. M. Wang, and H. E. Horng, Phys. Rev. B **59**, 8956 (1999).
[34]Y. Abulafia, A. Shaulov, Y. Wolfus, R. Prozorov, L. Burlachkov, Y. Yeshurun, D. Majer, E. Zeldov, H. Wühl, V. B. Geshkenbein, and V. M. Vinokur, Phys. Lett. **77**, 1596 (1996).
[35]Y. Yeshurun and A. P. Malozemoff, Phys. Rev. Lett. **60**, 2202 (1988).
[36]Xiao-Lin Wang, S. R. Ghorbani, Sung-Ik Lee, S. X. Dou, C. T. Lin, T. H. Johansen, K.-H. Müller, Z. X. Cheng, G. Peleckis, M. Shabazi, A. J. Qviller, V. V. Yurchenko, G. L. Sun, and D. L. Sun, Phys. Rev. B **82**, 024525 (2010).
[37]C. P. Bean, Rev. Mod. Phys. **36**, 31 (1964).
[38]R. Jin, M. Paranthaman, H. Y. Zhai, H. M. Christen, D. K. Christen, and D. Mandrus, Phys. Rev. B **64**, 220506 (2001).
[39]J. Luo, T. P. Orlando, J. M. Graybeal, X. D. Wu, and R. Muenchausen, Phys. Rev. Lett. **68**, 690 (1992).
[40]A. V. Samoilov, Phys. Rev. Lett. **71**, 617 (1993).
[41]A. T. Dorsey and M. P. A. Fisher, Phys. Rev. Lett. **68**, 694 (1992)
[42]V. M. Vinokur, V. B. Geshkenbein, M. V. Feigel'man, and G. Blatter, Phys. Rev. Lett. **71**, 1242 (1993).
[43]R. C. Budhani, S. H. Liou, and Z. X. Cai, Phys. Rev. Lett. **71**, 621 (1993).
[44]W. N. Kang, B. W. Kang, Q. Y. Chen, J. Z. Wu, S. H. Yun, A. Gapard, J. Z. Qu, W. K. Chu, D. K. Christen, R. Kerchner, and C. W. Chu, Phys. Rev. B **59**, R9031 (1999).
[45]N. B. Kopnin and G. E. Volovik, Phys. Rev. Lett. **79**, 1377 (1997).
[46]G. D'Anna, V. Berseth, L. Forró, A. Erb, and E. Walker, Phys. Rev. B **61**, 4215 (2000).
[47]P. W. Anderson, Phys. Rev. Lett. **67**, 2092 (1991).
[48]Gang Xiao, Peng Xiong, and Marta Z. Cieplak, Phys. Rev. B **46**, 8687 (1992).
[49]Peng Xiong, Gang Xiao, and X. D. Wu, Phys. Rev. B **47**, 5516 (1993).
[50]L. M. Wang, H. C. Yang, and H. E. Horng, Phys. Rev. B **56**, 6231 (1997).
[51]Z. D. Wang and C. S. Ting, Phys. Rev. B **46**, 284 (1992)
[52]Terukazza Nishizaki, Takafani Anmine, Itsuhiro Fujii, Kazunaki Yamamoto Shizuka Yoshii, Takahito Terashima, and Yoshichika Banso, Physica C **181**, 223 (1991).
[53]Z. X. Gao, E. Osquiguil, M. Maenhoudt, B. Wuyts, S. Libbrecht, and Y. Bruynseraede, Phys. Rev. Lett. **71**, 3210 (1993).